

SPECTROPOLARIMETRY AND THE NATURE OF NGC 1068

R. R. J. ANTONUCCI

National Radio Astronomy Observatory,¹ Charlottesville

AND

J. S. MILLER

Lick Observatory

Received 1985 February 1; accepted 1985 April 17

ABSTRACT

Extensive high-resolution, high signal-to-noise ratio polarization spectra of the nucleus of NGC 1068 are presented. The nonstellar continuum is polarized $\sim 16\%$, independent of wavelength. We have discovered broad Balmer lines and Fe II emission, with polarization $\gtrsim 15\%$ at approximately the same position angle as that of the continuum. The polarized flux spectrum closely resembles the flux spectrum of Seyfert type 1 nuclei. We conclude that the continuum and broad-line polarization is due to scattering, probably by free electrons. For NGC 1068, as well as apparently for all other Seyfert 2 galaxies, the optical polarization position angle is perpendicular to the nuclear symmetry axis as determined by the radio morphology. We suggest that the continuum and broad-line emission regions are located inside an optically and geometrically thick disk. Continuum and broad-line photons are scattered into the line of sight by free electrons above and below the disk. The narrow-line region and the thermally emitting nuclear dust clouds have a more direct view of the continuum source, explaining why they seem too strong to be powered by the observed continuum.

The narrow lines seen in the flux spectrum all have similar low polarizations, including the narrow Balmer lines. There is no evidence that the narrow Balmer lines and the [O III] lines come from qualitatively different regions, despite earlier suggestions to the contrary. Both P and θ vary with wavelength within the profile of the [O III] $\lambda 5007$ emission line. Therefore, the velocity field in the spatially unresolved narrow-line region is organized and not chaotic. The polarization variations may mean that the spatially resolved velocity field, reported by Walker in 1968, indicating expansion of narrow-line clouds in the plane of the host galaxy, extends into the unresolved region.

Subject headings: galaxies: individual — galaxies: nuclei — galaxies: Seyfert — polarization

I. INTRODUCTION

When broad-band polarization of the light of Seyfert nuclei was first studied, it was taken as evidence for optical synchrotron radiation (e.g., Walker 1968; Visvanathan and Oke 1968). The fact that polarization generally decreases with wavelength was attributed to wavelength-dependent dilution by unpolarized starlight.

The first good (low-resolution) spectropolarimetry data were reported by Angel *et al.* (1976). They studied NGC 1068, the subject of this paper. They found that the Balmer lines were polarized like the neighboring continuum, and that the forbidden lines were polarized differently. They also made the first and only detection of optical circular depolarization of an active nucleus. Their conclusion was that the continuum linear polarization *intrinsically* decreased with wavelength, and that it was caused by scattering of nuclear light by small dust grains. A final result from this paper was that the Balmer lines were polarized differently from the forbidden lines in this Seyfert 2 nucleus, implying that they came from a different region. This was surprising, since the profiles are all similar.

With higher resolution spectrophotometry and spectropolarimetry data, we found that, even using a small aperture, the light is dominated by unpolarized starlight. After correction for this, the nuclear polarization is seen to be very high and

wavelength-independent (Miller and Antonucci 1983, hereafter Paper I). McLean *et al.* (1983) came to the same conclusion independently. In Paper I we concluded that either a synchrotron radiation or electron scattering origin was likely for the continuum polarization. Both Paper I and McLean *et al.* (1983) also reported two additional interesting effects. First, the polarization varies across the profile of the [O III] $\lambda 5007$ line. Second, $P(\lambda)$ shows structure including excesses just redward of each Balmer line. In this paper we present the details of our observations, including many data not shown in Paper I. These data apparently resolve the dilemma of the cause of continuum polarization, and we interpret the structure in $P(\lambda)$ as revealing an important new aspect of NGC 1068. (A brief report of these new results appears in Antonucci and Miller 1984). We also present polarization measurements of many emission lines, and discuss the meaning of the wavelength-dependence of polarization within the $\lambda 5007$ line. In the Appendix we compare our polarization measurements with those of Angel *et al.* (1976) and McLean *et al.* (1983).

II. OBSERVATIONS

All of the observations were made with the Lick 3 m Shane telescope Image Dissector Scanner as modified for simultaneous spectrophotometry and spectropolarimetry by Miller, Robinson, and Schmidt (1980). The instrument measures the spectrum of the extraordinary and ordinary rays of both program object and sky simultaneously. The optical paths of

¹ National Radio Astronomy Observatory is operated by Associated Universities, Inc., under contract with the National Science Foundation.

the *E* and *O* rays are electronically modulated approximately every 2 s using a Pockels cell. The entrance apertures used for the object and for the sky are switched every 8 minutes. The system was designed for very low instrumental polarization and reliable spectrophotometry.

The observations were taken during eight nights between 1980 September 16 and 1980 December 14, always using a 2".8 circular aperture. Table 1 shows the observing log. The data set comes in four parts. First, Paper I and Figure 1 show the data taken with a 600 lines mm⁻¹ grating (resolution ≈ 10 Å) in the blue region of the spectrum. The 600 line grating, red-region data, which have higher signal-to-noise ratio, are shown in Figure 2. The H β , [O III] region was also observed with a 1200 lines mm⁻¹ (~ 5 Å resolution) grating (Fig. 3), as was the H α region (Fig. 4). All data were reduced and calibrated as discussed in Paper I and in Miller, Robinson, and Schmidt (1980).

III. THE POLARIZED FLUX SPECTRUM

a) General Continuum Properties

i) Descriptions of the Nonstellar Continuum

The continuum of NGC 1068 contains stellar and nonstellar light, and various attempts have been made to measure and characterize the different components. Table 2 shows several modern continuum flux measurements taken at or extrapolated to 5400 Å, along with the aperture size used. All of the direct determinations are mutually consistent. Starlight dominates all of the measurements. Our own measurement is probably the least accurate because of the small observing aperture.

The Meaburn *et al.* (1982) flux measurement was made using speckle interferometry. It is unexpectedly high. It is a very important measurement and we hope to see more speckle data on NGC 1068. Most of the flux in our 2".8 aperture is starlight. If it can be established that the flux which is unresolved by the speckle technique is comparable to the 2".8 scale flux, then substantial starlight must arise in an extremely compact region, perhaps in a "cusp" expected around a black hole.

The last two measurements in the table are power-law extrapolations from *IUE* data. (We have separated the short-wavelength camera and long-wavelength camera data from Neugebauer *et al.* 1980 because their Fig. 3 shows a discontinuity between the two.) The extrapolations predict more nonstellar flux at 5000 Å than we see total flux, so the *IUE* power law apparently does not extend unmodified into the visual region, or else it was subject to some calibration error. (Similarly, Malkan and Filippenko 1983 see pure starlight at 8500 Å, and they say this shows that a power law defined by Malkan and Oke 1983 in the blue must flatten in the far red.)

TABLE 1
OBSERVING LOG

Date (1980)	Spectral Region	Integration Time (minutes)	Resolution (Å)
16 Sep.....	Blue	128	10
9 Oct	Blue	128	10
10 Oct	H β	128	5
13 Nov.....	H β	128	5
14 Nov.....	Red	192	10
12 Dec	Red	176	10
13 Dec	H α	188	5
14 Dec	H α	128	5

TABLE 2
MEASUREMENTS OF THE CONTINUUM FLUX AT 5400 Å

Source	(0".03)	2".8	7"	10"	15"
This paper	1.8
Wampler 1971	6.5
Shields and Oke 1975	5.0
Neugebauer <i>et al.</i> 1980	11.6
Malkan and Filippenko 1983	1.3	4.2	6.7	10.8
Meaburn <i>et al.</i> 1982	6.5
Neugebauer <i>et al.</i> 1980 (<i>IUE</i> SW extrapolation)	2.9
Neugebauer <i>et al.</i> 1980 (<i>IUE</i> LW extrapolation)	4.5

NOTE.—Units are 10⁻¹⁴ ergs cm⁻² Å⁻¹. The Malkan and Filippenko 1983 data have been scaled from their 10" measurement by the aperture curve of growth of Malkan and Oke 1983. The Meaburn *et al.* 1982 measurement is by speckle interferometry. The *IUE* measurements use a large aperture but should be dominated by the nuclear nonstellar source.

Arbitrarily dereddening the *IUE* points does not reduce the extrapolated flux at 5400 Å; though dereddening flattens the slope of the *IUE* power law, it also raises the absolute level.

Several workers have fitted the continuum to a model consisting of a galaxy of stars plus a power law continuum. Malkan and Oke (1983) find that if $E_{B-V} = 0.10$ then the intrinsic power law spectral index is -1.1 . With this amount of dereddening, we can say their "observed power-law slope" is approximately -1.5 . Visvanathan and Oke (1968) found a power-law spectral index of approximately -1.5 for the polarized flux and suggested it was also applicable to the nonstellar flux in general. However, their polarization measurement errors were large. Koski (1978) suggested a spectral index of -1 , but this was not purely observational; he needed a power-law slope ≥ -1 to provide enough ionizing photons in his model calculations. Neugebauer *et al.* (1980) found $\alpha = -1.85$ based on *IUE* data, but if the data from the two cameras are kept separate they each suggest approximately -1.5 .

Our 2".8 aperture nonstellar flux (Paper I) was roughly proportional to ν^{-2} , but spectrum shapes obtained with a small aperture can be unreliable. Also, this estimate was affected by the emission we now attribute to Fe II (see § IIIb), so that the true nonstellar continuum in our data is actually somewhat bluer than this. We plan to measure the wavelength dependence of polarized flux with a large aperture. (Subtracting a galaxy component from a small-aperture scan to derive the wavelength dependence of nuclear polarization is not so dangerous. To the extent that the stellar light is spatially uniform, the small aperture does not affect the measured shape of the stellar spectrum. The power law from the point source is affected, but the polarized flux is affected exactly proportionately, so the derived wavelength dependence of nuclear polarization is unaffected.)

ii) Comments on the Circular Polarization of NGC 1068

This subsection is rather specialized, and the general reader may wish to skip it.

Angel *et al.* (1976) have shown that the light from NGC 1068 is slightly circularly polarized. It is the only extragalactic object with known optical circular polarization. The discoverers attributed it to multiple scattering within a dust cloud. We (Paper I) and McLean *et al.* (1983) suggested that it could result from the highly polarized continuum being *singly* scat-

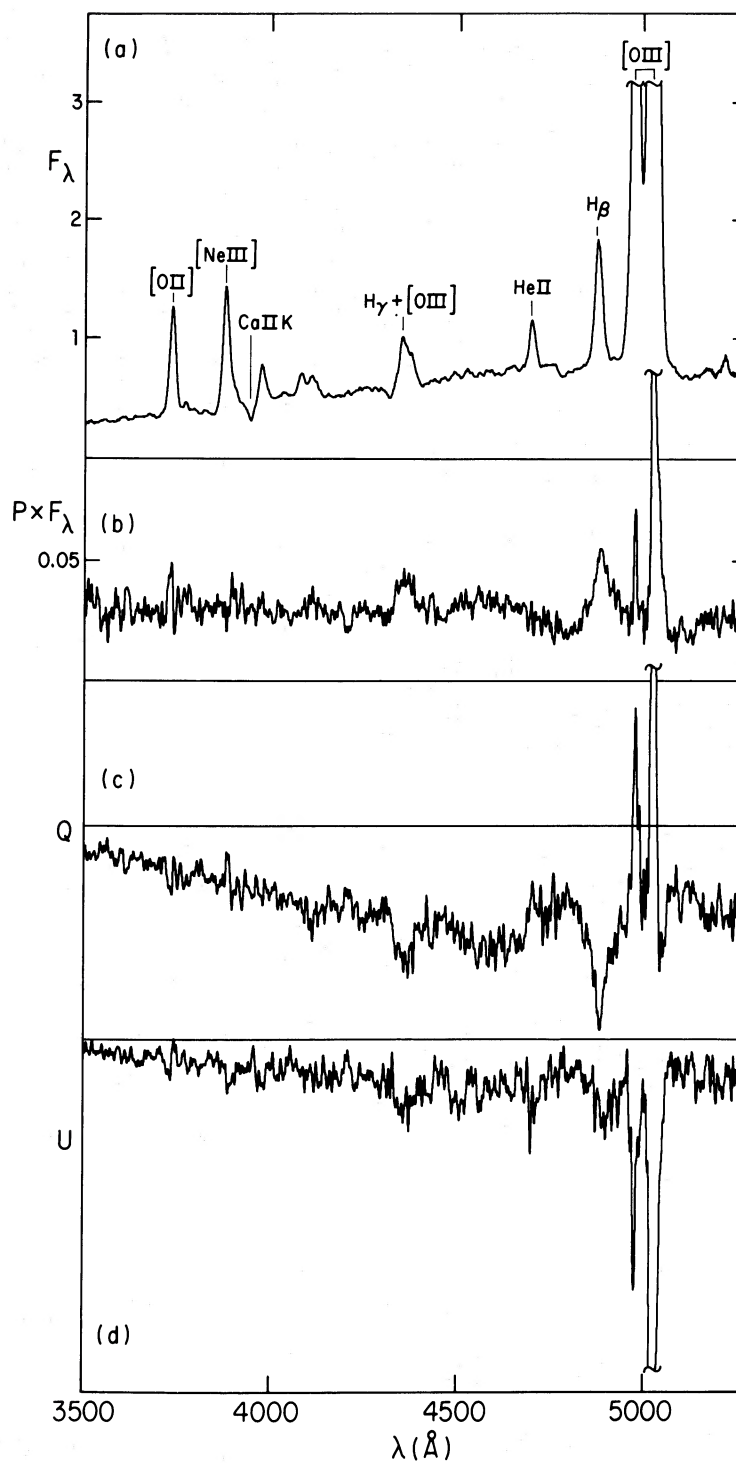


FIG. 1.—Flux, polarized flux, and Stokes parameter spectra in the blue region at 10 \AA resolution. The flux and polarized flux are in the same (arbitrary) units, so they can be compared directly. The Stokes parameters are in number of counts and have not been flux calibrated. The Q and U plots do have the same vertical scale.

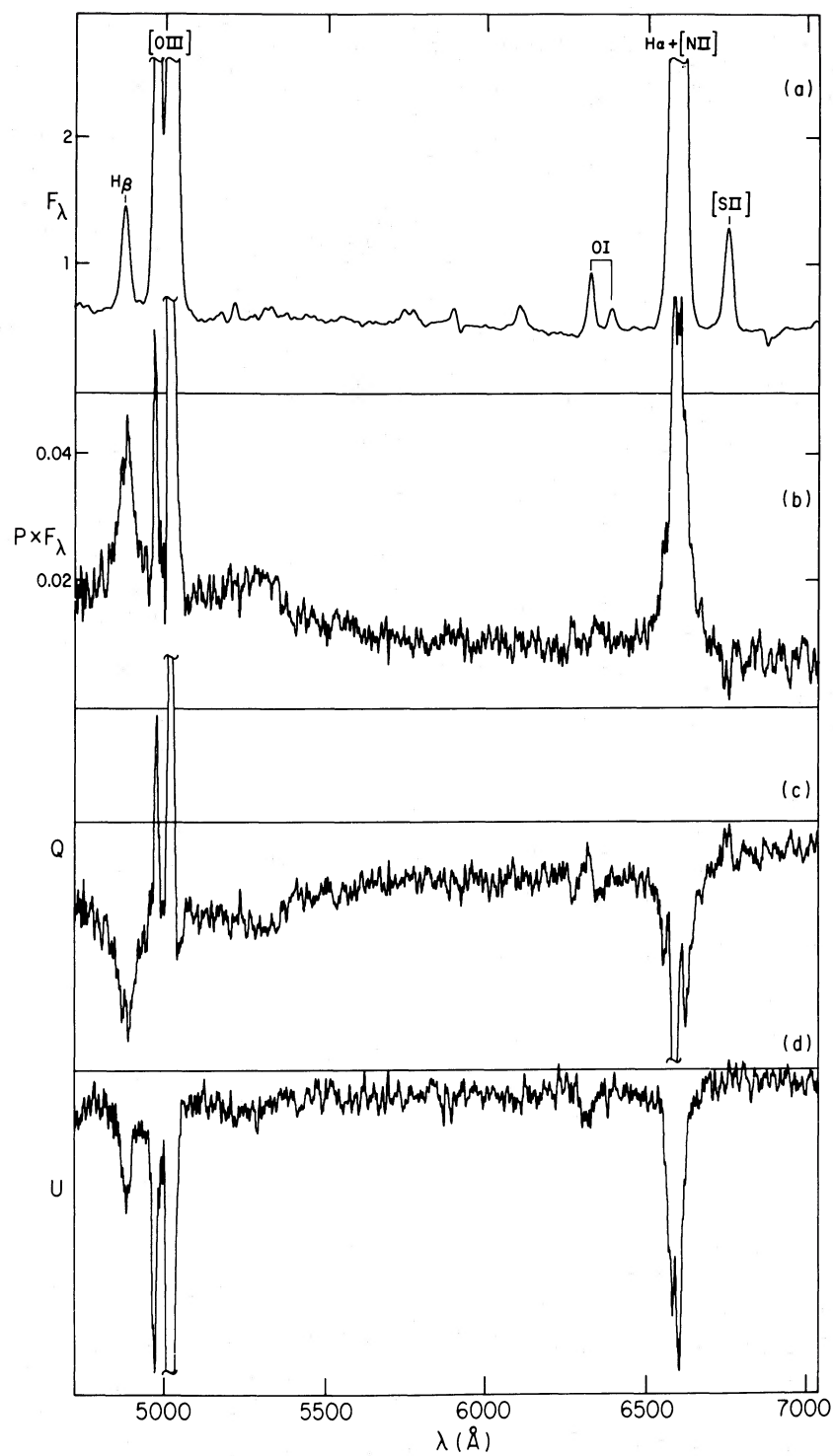


FIG. 2.—Same as Fig. 1, but in the red region

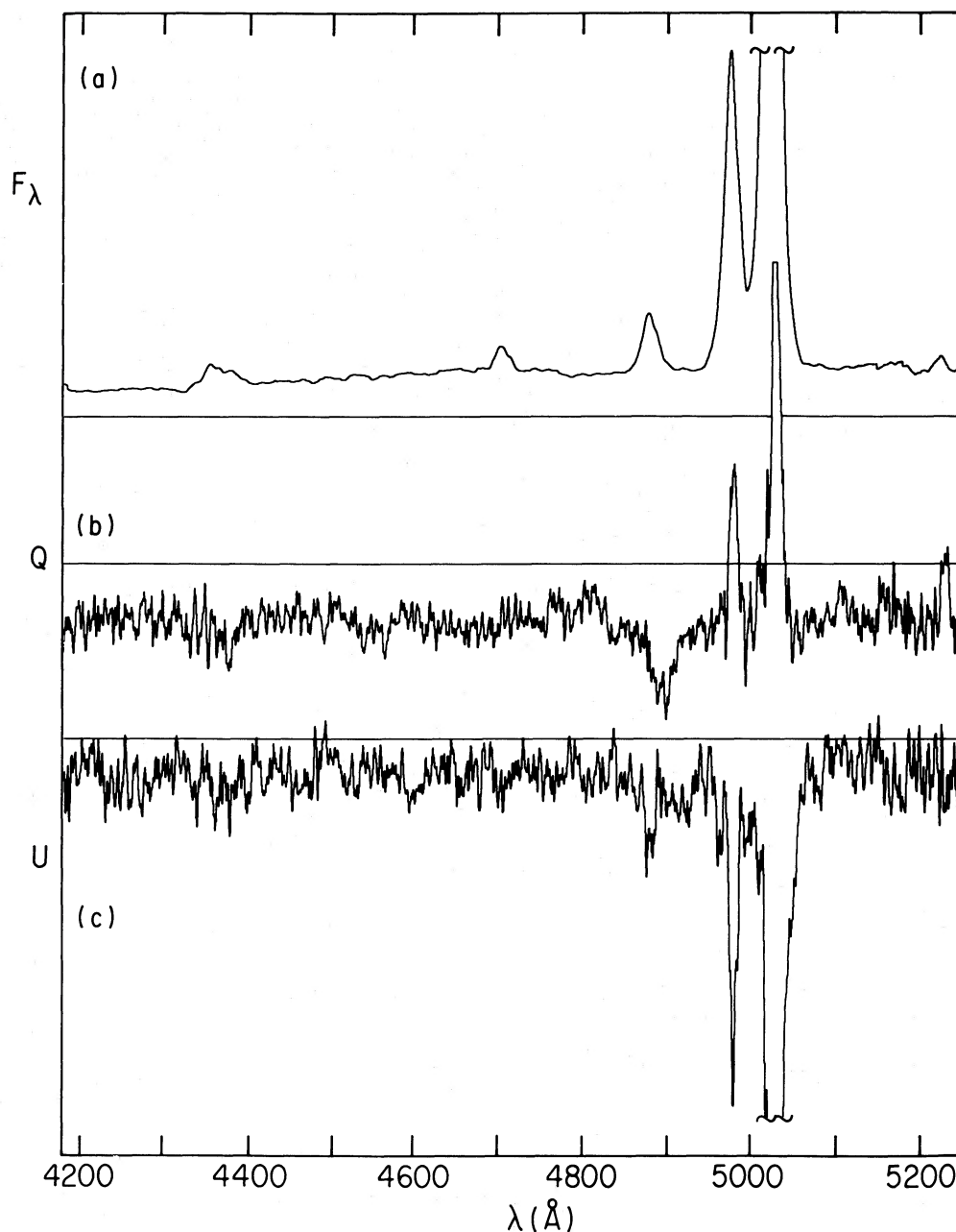


FIG. 3.—Flux and Stokes parameters in the H β , [O III] region at 5 Å resolution

tered by dust grains. Of considerable importance in understanding this phenomenon is the Angel *et al.* (1976) claim of detecting circular polarization in the narrow H α emission line. We present below a third possible explanation for the circular polarization which predicts that it occurs only in the continuum.

The ellipticity for the H α , [N II] blend quoted in the text of Angel *et al.* (1976) is $3.6\% \pm 1.2\%$, but according to their Table 2, this is a raw value (measured with an interference filter). In other words it includes the continuum underneath the lines. In the text the authors explicitly correct the linear polarization of this blend for the effects of the underlying continuum, but they do not do so for the circular measurement.

How much of the flux in this filter is due to the continuum?

Angel *et al.* (1976) do not say what value they used in correcting the linear polarization, but from their raw (line plus continuum), continuum, and line values we find that they must have used a continuum fraction $f_c = 0.30$. We will take this value and correct their circular measurement as follows. Let the percent circular polarization in the line, in the continuum, and in the line plus continuum be V_L , V_C , and V_{L+C} , respectively. Then

$$V_L = \frac{V_{L+C} - V_C f_c}{1 - f_c} = 0.020\% \pm 0.017\% .$$

Their detection of circular polarization in the line emission is therefore of only marginal significance.

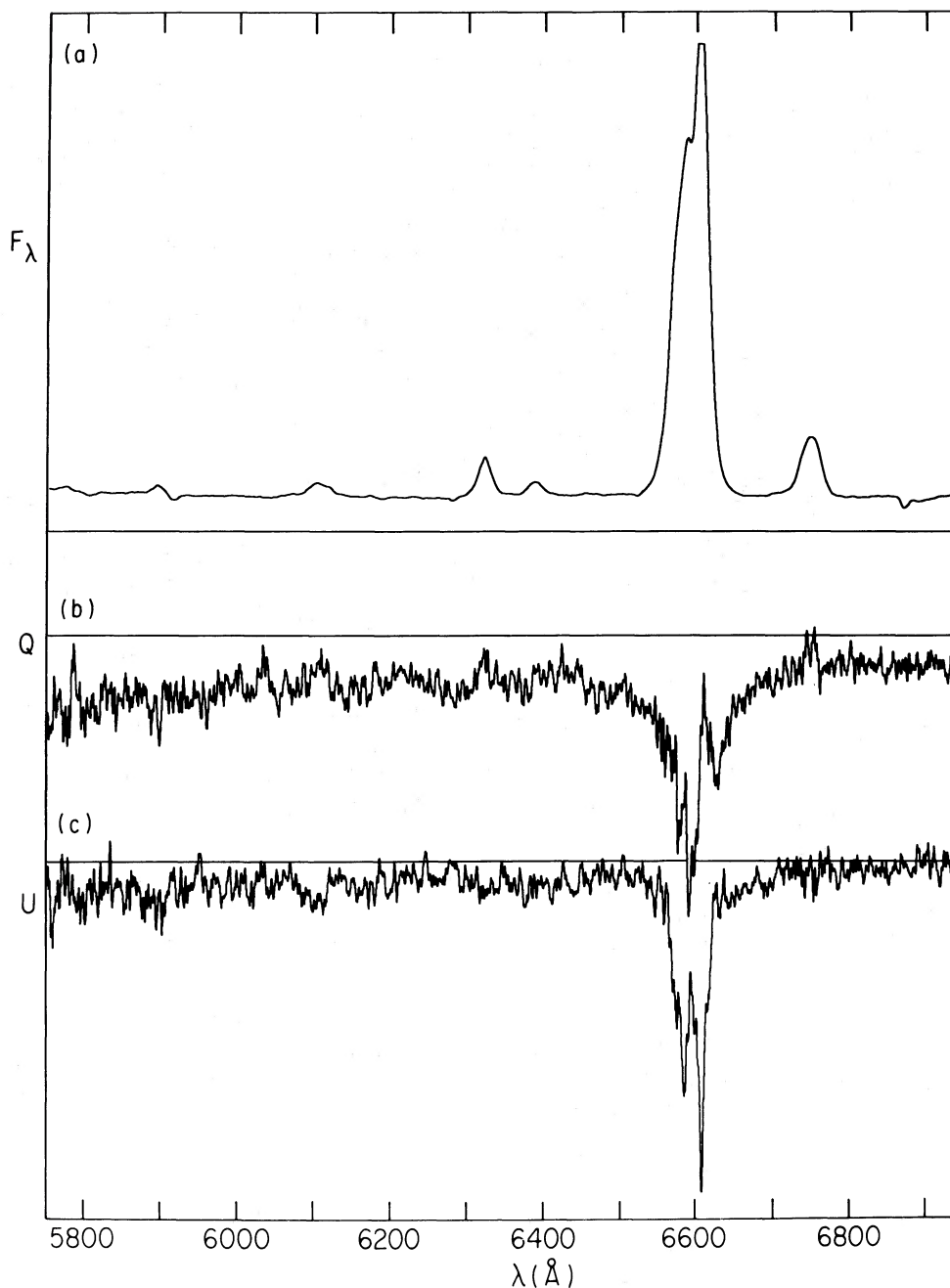


FIG. 4.—Flux and Stokes parameters in the H α , [N II] region at 5 Å resolution

We would like to propose a possible “radical” explanation for the continuum circular polarization. It is not central to our view of NGC 1068, but it may explain the circular polarization. The nonstellar linear polarization has been shown to be approximately wavelength-independent. Therefore, the linear rise in ellipticity to the red found by Angel *et al.* (1976) means there is a linear increase with wavelength in percent circular polarization.

It is obvious that there are (at least) two components to the nonstellar light from NGC 1068. Besides the optical/UV “power law,” there is thermal dust emission dominating the infrared. This dust emission is substantially linearly polarized (Lebofsky, Rieke, and Kemp 1978). No infrared circular

polarization measurements are known to us. We suggest that the optical circular polarization could have nothing to do with the optical/UV power law, but instead that it could be due to the tail end of the thermal dust emission. This idea appears radical because thermal dust emission is usually considered insignificant in the optical.

Let us discuss the two continuum components which remain after the starlight has been removed by subtraction. Suppose the optical power law is $F_\nu \propto \nu^{-1.5}$, and that it has 16% wavelength-independent linear polarization at a position angle of 95°. Assume the near-infrared dust emission comes from a single slab. For this order-of-magnitude calculation we assume the dust emission linear polarization is a constant 3% at 125°

after starlight subtraction (Lebofsky, Rieke, and Kemp 1978). The $2\ \mu\text{m}$ polarization position angle is $\sim 114^\circ$, part way between that of the IR component and that of the optical component, indicating that the polarized flux from the optical power law is somewhat less than that from the thermal dust emission. The dust would then account for $\sim 90\%$ of the total $2\ \mu\text{m}$ flux. What is the fraction of $0.4\ \mu\text{m}$ flux attributable to dust emission?

The Planck function at $0.4\ \mu\text{m}$ is 2×10^{-6} smaller than at $2\ \mu\text{m}$, if there is very hot dust emitting at a temperature of 1600 K. This is near the dissociation temperature for graphite grains. (Very hot dust does apparently exist in nature; e.g., Bergeat *et al.* 1976; The *et al.* 1981; Ney and Hatfield 1978. It may already have been detected in Seyfert galaxies, according to Rieke 1984.) This must be multiplied by the absorptivity ratio Q_r , which could be as high as 10^3 or 10^4 with $\sim 0.16\ \mu\text{m}$ radius particles (see the figures of Aannestad 1975). Now the optical power law is down by a factor of 11 at $0.4\ \mu\text{m}$. If the dust emission contributes 90% of the flux at $2\ \mu\text{m}$, these figures indicate that it may also contribute significantly at $0.4\ \mu\text{m}$. If we suppose that the dust provides $\sim 20\%$ of the $0.4\ \mu\text{m}$ non-stellar flux, it would need to be $\sim 2.5\%$ circularly polarized to agree with the observations, a high value, but possible. (Since the dust emission may well have a linear polarization at least as great as its circular value, it could also affect the observed linear polarization at least slightly.)

The flux ratio at the two wavelengths is only proportional to Q_r if the absorption optical depths are < 1 ; in order to get substantial circular polarization we need high scattering optical depths. According to Aannestad's figures, the absorption optical depth in the wavelength range of interest is similar to or somewhat larger than that at $500\ \mu\text{m}$. We know the absorption optical depth at $500\ \mu\text{m}$ is small because the spectrum is steeper than the Rayleigh-Jeans law there (Hildebrand *et al.* 1977). We know the scattering optical depth is large because the scattering cross section shortward of $1\ \mu\text{m}$ is comparable to or larger than the absorption cross section at $10\ \mu\text{m}$, and the absorption optical depth at $10\ \mu\text{m}$ is ~ 1 (Lebofsky, Rieke, and Kemp 1978). (Since the scattering optical depth in the $3\text{--}5\ \mu\text{m}$ region is small, there may be no circular polarization there.)

There are two consistency checks one can make. If the $10\ \mu\text{m}$ absorption optical depth is ~ 1 , then the dust flux at $0.4\ \mu\text{m}$ cannot greatly exceed the Planck function value at the assumed grain temperature, normalized to the $10\ \mu\text{m}$ point. Also, it should not be much less than the Planck value because the absorption optical depth at $0.4\ \mu\text{m}$ should not be very small; the absorption cross section is similar to that at $10\ \mu\text{m}$. At $10\ \mu\text{m}$, $F_\nu \approx 20\ \text{Jy}$ in a $\sim 5''$ aperture (Rieke and Low 1975) and

$$\frac{B_\nu(1600\ \text{K}, 0.4\ \mu\text{m})}{B_\nu(1600\ \text{K}, 10\ \mu\text{m})} = 6.5 \times 10^{-6},$$

so we expect $F_\nu(0.4\ \mu\text{m}) < 0.13\ \text{mJy}$. At $0.4\ \mu\text{m}$ the observed flux in a $2''$ aperture is $\sim 4\ \text{mJy}$ including the starlight (Malkan and Oke 1983, Fig. 1). In order to account for the $\sim 0.1\%$ circular polarization in a $2''$ aperture, we would like $\sim 5\%$ of this to be hot dust emission, that is $\sim 0.2\ \text{mJy}$. This is acceptable agreement.

Another consistency check can be made using the Planck surface brightness. The $0.4\ \mu\text{m}$ dust surface brightness is less than or equal to the Planck surface brightness. We want $F_\nu \approx 0.2\ \text{mJy}$, and this corresponds to an optically thick dust cloud

of angular size ~ 10 milli-arcsec. This would not be in conflict with any other observation. We could distinguish between this explanation for the circular polarization and that of Paper I (and McLean *et al.* 1983) by a definitive measurement of the broad Balmer line circular polarization.

b) Structure in the Polarization Spectrum: The Seyfert 1 inside NGC 1068

There is a great deal of structure in the polarization spectrum. As explained in Paper I, much of it is due to dilution of a featureless continuum by unpolarized starlight. We see many stellar absorption lines "in emission" in the polarization spectrum, because there is less starlight reducing P at those wavelengths. Similarly we can see the stellar continuum breaks in $P(\lambda)$. As we noted in Paper I, $P(\lambda)$ really looks like a galaxy spectrum plotted upside down.

There are some polarization features that cannot be explained by dilution. We noted in Paper I that there is a polarization excess redward of each narrow Balmer line, and in studying our data more carefully, we also see small excesses in P blueward of $H\alpha$ and $H\beta$. There is also excess polarization in the $4500\text{--}4600\ \text{\AA}$ region. McLean *et al.* (1983) find similar structure in $P(\lambda)$. Interpretation of these features appears to provide the key to the NGC 1068 polarization, and it is the most important part of this paper.

Plots of polarized flux, $P(\lambda) \times F(\lambda)$, eliminate the effects of unpolarized starlight, and suppress low-polarization line emission. Figures 1 and 2 show the polarized flux, and the appearance of these figures is surprising. They look like the spectra of a Seyfert Type 1 object! Broad symmetric Balmer lines and Fe II emission are clearly seen. The Balmer line full widths at zero intensity are $\sim 7500\ \text{km s}^{-1}$. The presence of Fe II is crucial in establishing that this broad emission comes from clouds of very high optical depth. We can draw several rather secure conclusions from these plots. First, there are (broad) emission lines with polarization magnitude and position angle similar to that of the continuum. This follows from the fact that they do not show strongly in the $\theta(\lambda)$ or starlight-corrected $P(\lambda)$ plots (Paper I). Their polarization must be due to scattering. The natural inference from the fact that the nonstellar continuum and the broad lines have similar values of P and θ is that both are polarized by the same mechanism. We can conclude that the wavelength-independent polarization of the continuum light is almost certainly due to electron scattering rather than synchrotron radiation. We also know that the temperature of the electrons is $< 10^6\ \text{K}$; otherwise the lines would be thermally broadened by an amount greater than their observed width.

With hindsight we can barely see the Fe II and broad wings of $H\beta$ in our starlight-subtracted total flux plot (Paper I), especially as excess flux between the narrow $H\beta$ line and [O III] $\lambda 4959$. The excess appears in the coudé spectrum of Malkan and Filippenko (1983, Fig. 3). They spotted it and noted in their Appendix that "H β may have a very faint broad component."

There is a close analogy between NGC 1068 and the radio galaxy 3C 234 (Antonucci 1984). Both have very high wavelength-independent continuum polarization, highly polarized broad Balmer emission, and low-polarization narrow lines. In a plane-parallel electron-scattering atmosphere, P can never exceed 11.7% , even if the plane is edge-on such as the limb of a B star (Chandrasekhar 1946). For this reason we concluded (Antonucci 1984) that the $\sim 14\%$ polarization of the

radio galaxy 3C 234 implied that the continuum source and broad-line region are hidden deep inside a thick disk. We see only those continuum and broad-line photons which travel out the polar directions and scatter into the line of sight. The disk would have to be perpendicular to the radio structure axis to account for the perpendicular polarization alignment. The scattering medium would have to be optically thin to account for the high polarization. As we suggested in Paper I, such a picture is suitable for NGC 1068 as well. In both cases the extrapolation of the observed nonstellar continuum is insufficient to account for either the narrow line emission or the thermal dust emission in the near-infrared (Neugebauer *et al.* 1980). If the narrow line and nuclear dust emission regions are both powered by the nuclear source, both regions must have a more direct view of the nucleus than we do. For both NGC 1068 and 3C 234, we only see an electron-scattered image of the continuum emission and broad-line regions. This picture may be valid for all Seyfert 2 galaxies, since they all apparently show optical polarization position angles perpendicular to the nuclear symmetry axes as determined by the radio morphology (Antonucci 1983, 1984).

Figure 5 shows the geometrical configurations which we are proposing. We have drawn a mysterious central continuum source surrounded by a very thick absorbing disk. It is possible that the continuum source is a small radiating accretion disk which is really just a flat inner extension of the large disk in the drawing. In other words the radiating accretion disk may flare

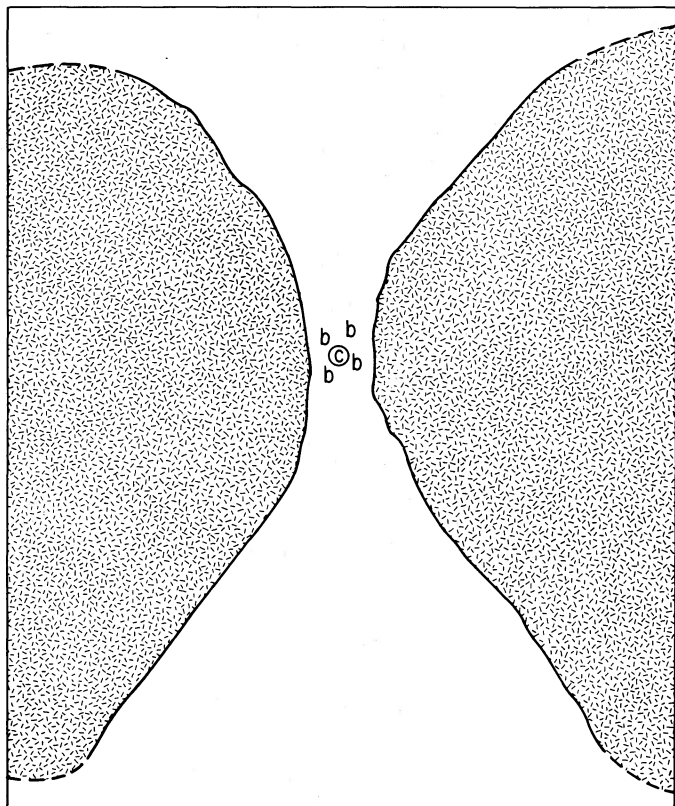


FIG. 5.—Cutaway drawing of a continuum source and broad-line clouds surrounded by a geometrically and optically thick disk. Only photons traveling out along the polar directions can scatter into the line of sight. We would observe a high polarization in the plane perpendicular to the symmetry axis, which we presume to be the radio structure axis.

out and extend to very large distances (parsecs?) from a central black hole.

With this new insight about the highly polarized broad lines, we can resolve a mystery about the narrow line region. In Seyferts of Type 2 (Koski 1978) and also of Type 1.5 (Cohen 1983), the ratio of the $[\text{O III}] \lambda 5007$ line flux to that of narrow $\text{H}\beta$ is generally around 10. In at least one Seyfert 1.5 (NGC 4151; see Schmidt and Miller 1980), spectropolarimetry data indicate that the two lines probably come from the same region. Low-resolution spectropolarimetry of NGC 1068 (Angel *et al.* 1976) appeared to show that narrow $\text{H}\beta$ does not originate in the $[\text{O III}]$ region. If this is the case, why does NGC 1068 have a narrow line ratio like a Seyfert 1.5? If most of the narrow $\text{H}\beta$ comes from a region distinct from the $[\text{O III}]$ region, the $\lambda 5007/\text{narrow H}\beta$ ratio in the $[\text{O III}]$ region must be extremely high. How would we explain such a high ratio theoretically?

It is clear from our plots of the Stokes parameters that most of the polarized flux not attributable to the continuum at the wavelength of the narrow Balmer lines comes from the hidden broad lines. Therefore, the raw polarization of the narrow lines does not reveal anything about the location of the narrow Balmer line clouds. Consider the high S/N medium-resolution red Q plot, Figure 2c. The forbidden lines of $[\text{O III}]$ show a swing toward positive Q values, since their position angle is $\sim 155^\circ$. At $\text{H}\beta$, where there are no forbidden lines complicating the plot, we can see that the effect of the narrow $\text{H}\beta$ line is qualitatively the same as the forbidden lines (Fig. 2c). The same effect is probably present for the heavily blended $[\text{N II}]$ and narrow $\text{H}\alpha$ lines cutting into the broad $\text{H}\alpha$ profile. (Here the high-resolution data of Fig. 4 are required to see what is going on.) The polarization data are entirely compatible with the assertion that the narrow $\text{H}\beta$ line arises in the region emitting the $\lambda 5007$ line. (This appears to be true of Mrk 3 as well despite the suggestions of Thompson *et al.* 1980 and Schmidt and Miller 1985 to the contrary; improved spectropolarimetry of Mrk 3 has been obtained by Miller [J. S. Miller, in preparation].)

Note that the narrow line is blueshifted slightly with respect to the broad line. This is why the excess polarization in the raw $P(\lambda)$ spectrum occurs mainly redward of the narrow line. The broad-line peak is displaced roughly 600 km s^{-1} to the red of the narrow line. The relative redshift of the broad components could mean that the scattering electrons are moving away from the emitting clouds, perhaps because the whole system is in expansion. Other explanations such as a gravitational redshift are conceivable. The existence of the broad Fe II emission shows that the broad-line clouds have high optical depths, and so are analogous to those in Seyfert 1 galaxies and QSOs.

Generally speaking, these observations tell us something about the nature of the nonstellar continuum in NGC 1068 and perhaps other Seyfert 2 galaxies, as documented by Koski (1978). Our polarized flux plots suggest that *the continuum is essentially the same phenomenon as the continua of Seyfert 1 galaxies.*

The flat decrement, which we estimate as $P \times F$ (broad $\text{H}\alpha$)/ $P \times F$ (broad $\text{H}\beta$) = 2.2 ± 0.4 , may indicate a high value of the ionizing photon density (e.g., Kwan 1984). (This is usually parameterized as $N_0 \times \Gamma$, the atomic density times the ionization parameter.)

At the suggestion of M. Ward, we have considered the relationship of the broad line emission to the X-ray emission. Seyfert 1 galaxies and optical QSOs show a tight correlation

between $H\beta$ broad-line luminosity and soft X-ray luminosity (e.g., Blumenthal, Keel, and Miller 1982). We have estimated the broad $H\beta$ flux of NGC 1068 by assuming the broad emission is $\sim 20\%$ polarized, which should be good to a factor of 2. The broad $H\beta$ flux is then ~ 0.017 times that of the $[O\text{ III}] \lambda 5007$ line. Taking the X-ray luminosity in the 0.5–4.5 keV band and the $\lambda 5007$ luminosity from Lawrence and Elvis (1982), we have plotted NGC 1068 on Figure 4 of Blumenthal, Keel, and Miller (1982). It does lie on the correlation line for radio-quiet objects. Since the broad-line emission is scattered into the line of sight and has a “normal” relationship to the apparent X-ray luminosity, one may suppose that the latter is also scattered into the line of sight in the same way. The X-ray source would not be seen directly under this hypothesis, perhaps explaining why Seyfert 2 galaxies are known to be weak X-ray emitters (Antonucci 1984). The X-rays from NGC 1068 would then be polarized $\sim 20\%$, in the plane perpendicular to the radio axis, just as the optical light is. A problem with this interpretation of the X-ray emission is that familiar astrophysical plasmas are better absorbers than scatterers of X-rays.

There is no secure way to estimate the electron scattering optical depth. Very large values would probably result in lower polarization. Very small values would imply that we are seeing only a tiny fraction of the total flux, which seems unlikely given that the narrow-line strengths are only around an order of magnitude greater than that expected from the observed continuum flux. It is interesting to note that the equivalent widths of narrow lines relative to the observed nonstellar continua are about 7 times larger in Seyfert 2 galaxies than in Seyfert 1 galaxies (Shuder 1981), again suggesting that we may be observing about one-tenth the full nonstellar flux in the Seyfert 2 galaxies. To get a feeling for the number of electrons needed for an electron-scattering optical depth of 0.1, consider the possibility that the electrons are in pressure equilibrium with broad-line clouds at $T = 10^4$ K, $N = 10^{9.5} \text{ cm}^{-3}$.² We know from the polarized-flux line widths that the electron temperature is $< 10^6$ K. Using $T_e = 10^5$ K, for pressure equilibrium $N_e = 10^{8.5} \text{ cm}^{-3}$. Since the Thomson cross section is $7 \times 10^{-25} \text{ cm}^2$, a column of length $4.4 \times 10^{14} \text{ cm} = 1.6 \times 10^{-4} \text{ pc}$ would have an electron-scattering optical depth of 0.1. We emphasize that these are *not* estimates for the parameters of the scattering material, but simply *illustrative* values. The temperature limit does indicate that the scattering medium is not a Comptonized plasma in thermal equilibrium.

If the electron-scattering optical depth is really only 0.1, perhaps from the polar directions we could observe the continuum and broad-line flux directly and we would classify this object as a Seyfert 1. A few Seyfert 1 galaxies could indeed be objects like NGC 1068 seen from a special direction, but this apparently cannot be the case for many of them. The reason is that the radio emission, which is almost certainly aspect-independent, is statistically very different in the two Seyfert classes (Ulvestad and Wilson 1984). Perhaps there is a correlation between radio properties and the *probability* that an object will be seen as a Seyfert 1. In our disk picture, both may be related to the disk opening angle.

IV. POLARIZATION OF THE NARROW EMISSION LINES

We have fairly good measurements of the polarization of many emission lines, integrated across their profiles, and we

have also measured the wavelength dependence of polarization within the lines of $[O\text{ III}]$. Aside from elementary physical and kinematic inferences, it is not obvious how to interpret this information.

Table 3 shows the line polarization measurements, with the associated statistical errors. The statistical errors are lower than the true errors for measurements of the strong lines, where calibration and continuum setting uncertainties predominate. We do not tabulate the narrow Balmer line polarizations here, since they are contaminated by polarized flux from the highly polarized broad lines as discussed in § III. To within the accuracy of the data, the Stokes parameter plots show the narrow Balmer lines are polarized like the forbidden lines.

The forbidden line polarization magnitudes are all generally 1%–2%, but they show some differences. The differences are not a simple function of the ionization potential or critical density of the emitting ions, or of the wavelength of the lines. Similarly, the position angles are not simple functions of either of those parameters. There is a tendency for forbidden lines with large polarizations to have lower position angles. The only direct conclusion from this is that all of the forbidden lines do not arise in exactly the same region, a result which was already obvious from studies of the emission-line spectrum (e.g., Shields and Oke 1975). The lack of a strong wavelength dependence suggests forbidden line polarization from dust transmission or electron scattering in the host galaxy, rather than from Rayleigh scattering by dust grains (Angel *et al.* 1976). We remind the reader that the emission lines are atop a continuum with substantial polarization structure, so all of the narrow-line measurements are somewhat suspect. It may be very significant that the $\lambda 5007$ line, which is extremely strong and therefore very reliably measured, definitely has a position angle along the host galaxy minor axis. This is also true of NGC 4151 (Schmidt and Miller 1980) and suggests that the unresolved narrow-line region is being influenced by the host galaxy.

Table 3 also shows the polarization in the core and wings of the $\lambda 5007$ line, with wavelength specified in the observer's rest

TABLE 3
POLARIZATION OF THE NARROW EMISSION LINES

Emission Lines	P	θ
[Ne v] $\lambda 3426$	1.11 ± 0.67	98.4 ± 16.9
[O II] $\lambda 3727$	1.45 ± 0.39	91.0 ± 7.5
[Ne III] $\lambda 3868$	0.85 ± 0.31	125.4 ± 10.2
[Ne III] $\lambda 3969 + \text{He}$	2.73 ± 0.69	108.1 ± 7.1
[S II] $\lambda \lambda 4068, 4076$	2.57 ± 0.82	90.4 ± 8.9
He II $\lambda 4686$	1.92 ± 0.23	166.3 ± 3.4
[O III] $\lambda 4959$	1.00 ± 0.04	145.7 ± 1.0
[O III] $\lambda 5007$	1.10 ± 0.02	142.0 ± 0.5
[O III] $\lambda \lambda 5001-5015$	0.65 ± 0.09	138.8 ± 4.1
[O III] $\lambda \lambda 5015-5035$	1.21 ± 0.04	143.3 ± 0.9
[O III] $\lambda \lambda 5036-5061$	1.70 ± 0.08	132.6 ± 1.3
[N I] $\lambda 5199$	4.56 ± 0.99	93.7 ± 6.1
[Fe VII] $\lambda 5721$	0.76 ± 0.89	118.4 ± 57
[N II] $\lambda 5755$	0.33 ± 0.72	121.9 ± 57
He I $\lambda 5876$	3.21 ± 0.58	107.6 ± 5.1
[Fe VII] $\lambda 6087$	1.54 ± 0.32	137.0 ± 5.8
[O I] $\lambda 6300$	1.20 ± 0.18	126.2 ± 4.2
[O I] $\lambda 6363$	1.53 ± 0.40	105.0 ± 7.3
[S II] $\lambda \lambda 6716, 6731$	0.36 ± 0.11	178.0 ± 8.6

NOTE.—Quoted uncertainties are based on count statistics only; true uncertainties are larger for strong lines. For the measurements within the $\lambda 5007$ profile only, wavelengths are specified in the observer's rest frame.

² Of course there is no reason to think this is the case. In fact there is no reason to think that the broad-line clouds in NGC 1068 have “normal” physical conditions.

frame. The variation across this line profile is the first proof that the velocity field in nuclear narrow line emission is organized and not chaotic. P rises monotonically with radial velocity, so that in some sense the clouds emitting the core of the line are "between" those emitting the blue wing and those emitting the red wing. The red wing has a lower position angle than the core, and the blue wing probably does too. If so, the clouds producing the two wings are somehow related spatially, and we argue below that they are located on a single geometrical line that passes through the nucleus.

Our search for the "Rosetta Stone" which would enable us to interpret position angles of forbidden line polarization lead us to a paper by Elvius (1978). She presents surface polarimetry of the region around the NGC 1068 nucleus, and her paper contains an interesting result. The off-nuclear polarization E -vectors are apparently *always perpendicular to the radius vector*. Her conclusion is that the off-nuclear polarization is due to nuclear light scattered by grains in the galaxy. The off-nuclear polarization is several percent, implying $\sim 10\%$ of the broad-band light is actually scattered nuclear light. Since the emission-line equivalent widths are much greater in the nuclear light than in the galaxy light away from the nucleus, the fraction of scattered nuclear light in the off-nuclear *emission lines* must be much larger than 10% . However, the off-nuclear emission lines actually tend to have rather different profiles and ratios than the nuclear lines have, so they are probably produced mostly locally in the galaxy (Walker 1968; Balick and Heckman 1979; Pelat and Alloin 1980), perhaps inconsistent with the explanation of scattered nuclear light for off-nuclear polarization. On the other hand, Elvius states that the off-nuclear polarization is mainly in the ultraviolet, favoring the scattered nuclear light idea. However, not much evidence for the wavelength-dependence of off-nuclear polarization is presented in Elvius' paper.

There is another possible interpretation for the "circumferential" off-nuclear position angles, which is consistent with the off-nuclear emission-line spectra being produced locally. The polarization may be due to dust transmission, and in this case the position angle would trace the magnetic field lines, that is to say probably the spiral arms. The arms are of course roughly circumferential. The problem with this idea is that it does not predict strong ultraviolet polarization. If the *nuclear forbidden line* polarizations are due to scattered light from nearer the exact center, or host galaxy dust transmission, it is likely that *their position angles indicate the direction orthogonal to the radius vector* from the predominant emitting or scattering cloud.

Similarly we may obtain some clues as to how to interpret the forbidden line profiles by considering data on the spatially resolved region around the core. Walker (1968) presented detailed kinematical evidence that the spatially resolved forbidden line clouds are both rotating and expanding in the galaxy plane. He found that for distances from the nucleus $r > 30''$ the velocity field is circular with the line of nodes at 55° , the same as the major axis direction of the inner spiral arms. For $r < 30''$ the radial velocity extrema are at 110° . The inner cloud velocities are greater than the escape velocity from the inner region (determined from the circular velocities at $r > 30''$), so they are not in rotation. They are not purely in expansion in the galaxy plane either because in that case the radial velocity extrema would be along the minor axis. Walker concluded that their motions are a combination of planar rotation and planar expansion.

What would we expect from the polarization as a function of wavelength within a forbidden line with this velocity field, under the assumption of locally produced emission lines polarized by dust transmission? If the trend toward increasingly radial (planar) velocities continues in toward the nucleus, then we would expect that our line center is produced along the major axis, by clouds moving in the sky plane. It has been argued that the polarization position angle will be perpendicular to the radius vector for each emitting cloud, so we would expect a core position angle along the minor axis of the galaxy, as in fact seen in the $\lambda 5007$ line. Perhaps the observation that *both* wings show position angle rotation in the same sense implies that they are emitted on one line passing through the nucleus. This is expected from planar expansion. The higher polarization of the red wing could relate to its being produced on the far side of the galaxy in this scenario.

In the explanation of scattered nuclear light for the line polarizations, we would expect θ and perhaps P to vary in the same way as in the previous picture, but the line center of gravity would be displaced to the red. The emission lines are known to be slightly blueshifted relative to the stellar absorption feature (Walker 1968), but the $[\text{O III}]$ lines in *polarized flux* are redshifted relative to the $[\text{O III}]$ lines in total flux. This could imply that the scatterings both polarize and redshift the line photons, as expected under this hypothesis.

These explanations for the polarization variation within the $[\text{O III}]$ $\lambda 5007$ profile have many loose ends. Why is the core position angle close to the integrated profile position angle? Why is the integrated polarization different for different forbidden lines? Why is the integrated polarization of the best-measured forbidden line, $\lambda 5007$, parallel to the minor axis both in NGC 1068 and in NGC 4151 (Schmidt and Miller 1980)? We need off-nuclear spectropolarimetry to help answer these questions and to determine the origin of the off-nuclear polarization.

V. CONCLUSIONS

1. From Paper I and from McLean *et al.* (1983), the polarization of the nuclear nonstellar continuum is very high and wavelength-independent.

2. The polarized flux plot reveals the presence of very highly polarized, very broad ($\sim 7500 \text{ km s}^{-1}$) symmetric Balmer lines and also permitted Fe II. This plot closely resembles the flux spectra of Seyfert type I nuclei. The broad lines are redshifted $\sim 600 \text{ km s}^{-1}$ relative to the narrow lines. This line emission, polarized qualitatively like the continuum, indicates that both polarizations are due to scattering, probably by free electrons. The electrons must be cooler than 10^6 K . NGC 1068, like apparently all Seyfert 2 galaxies (Antonucci 1983, 1984), has its optical polarization position angle perpendicular to the nuclear symmetry axis as determined by the radio map. We favor an interpretation in which the continuum source and broad line clouds are located inside a thick disk, with electrons above and below the disk scattering continuum and broad line photons in to the line of sight. This is the picture proposed by Antonucci (1984) to explain similar polarization data for the radio galaxy 3C 234. It accounts for the fact that the observed optical continuum is too weak to produce the narrow Balmer lines and the thermal dust emission.

3. All of the narrow lines, including the narrow Balmer lines, have similar low polarizations, unrelated to that of the continuum.

4. P increases to the red within the $[\text{O III}] \lambda 5007$ line. The position angle is lower in the red wing than in the core, and probably is also lower in the blue wing than in the core. Therefore the velocity field in the unresolved narrow line region is organized in some way. The data are consistent with Walker's (1968) planar expansion/rotation velocity field extending into

the unresolved nucleus, but such an interpretation is not unique.

Partial support for this work was provided by NSF grants AST 80-19322 and AST 84-06843. We would like to thank S. A. Stephens for making the plots shown in this paper.

APPENDIX

A COMPARISON OF THE PUBLISHED POLARIZATION DATA FOR NGC 1068

Spectropolarimetry is a new field, so it is important to establish whether the data are really reliable, or whether unknown systematic errors may enter in. Here we compare our continuum and line polarization data with those of Angel *et al.* (1976) and McLean *et al.* (1983). Apertures used are 2".8 circular, 2".0 circular, and 2".2 \times 1".7 rectangular, respectively.

Table 4 shows approximate continuum polarization measurements taken from published figures. We used the smooth curve drawn by Angel *et al.* through their data, and we drew a similar smooth curve through the McLean *et al.* data. The curve through our data is less smooth because our S/N is high enough to see, for example, the reflection of the stellar continuum breaks. Because the curves are drawn somewhat subjectively, we do not expect perfect agreement.

The agreement between the continuum data sets is only fairly good. Percent polarization is sensitive to the amount of dilution by unpolarized starlight, and therefore to seeing and guiding differences. Regarding position angle, we find $94^\circ < \theta < 96^\circ$ throughout the range $3500 \text{ \AA} < \lambda < 7000 \text{ \AA}$. The Angel *et al.* Digicon data plot looks consistent with $\theta = 100^\circ$ for $3300 \text{ \AA} < \lambda < 6600 \text{ \AA}$. Their filter data, which they apparently consider to be more reliable, indicate $\theta = 96^\circ$ in the $6000 \text{ \AA} < \lambda < 7400 \text{ \AA}$ continuum, and higher values in the blue. (Their blue filter passbands include strong forbidden lines.) The McLean *et al.* figure shows position angle very nearly constant at 100° . Our position angle zero point is based on observations during the same runs of the polarization standards Hiltner 102 and VI Cyg star 12 = Hiltner 992, assumed to have position angles of 75° and 118° , respectively (Hiltner 1956; Kruszewski 1971). The two standards gave position angle calibrations which agreed to within 1° .

Only Angel *et al.* and this paper list the polarization of many different emission lines. Polarization of a feature is determined by comparing the emission-line flux in a fixed wavelength interval to the continuum-corrected polarized emission in the same interval. We showed in § IIIb that such a process can lead to spurious results for the Balmer lines, because the polarized line flux can be unrelated to the narrow flux feature. It is also dangerous because the continuum polarization has so much structure. However, here our purpose is just to test the data sets, so we compare all of the Angel *et al.* apparent line polarization measurements to ours in Table 5.

In general the agreement is fairly good, though not quite as good as the purely statistical errors would indicate. Similarly the internal agreement within our data sets is a little worse than expected from counting statistics alone. One line, He II $\lambda 4686$, has poor

TABLE 4
CONTINUUM POLARIZATION COMPARISON

Continuum	Angel <i>et al.</i> 1976 (percent)	McLean <i>et al.</i> 1983 (percent)	This Paper (percent)
P_c (3700).....	7.0	...	8.0
P_c (4200).....	4.2	6.6	5.2
P_c (5500).....	1.4	1.8	2.3
P_c (6500).....	0.5	1.6	1.9

TABLE 5
EMISSION LINE POLARIZATION COMPARISON

LINE	ANGEL <i>et al.</i> 1976		THIS PAPER	
	Q	U	Q	U
[Ne v] $\lambda 3426$	-0.4 ± 2.3	-3.3 ± 2.6	-1.2 ± 0.4	-0.4 ± 0.7
[O II] $\lambda 3727$	2.2 ± 1.0	0.0 ± 1.1	-1.5 ± 0.4	-0.1 ± 0.4
[N III] $\lambda 3869$	-0.3 ± 0.8	-1.7 ± 0.9	-0.3 ± 0.3	-0.9 ± 0.3
H γ	-4.5 ± 1.3	0.0 ± 1.3	-3.4 ± 0.3	-1.7 ± 0.3
He II $\lambda 4686$	-2.5 ± 2.1	1.8 ± 1.9	1.7 ± 0.2	-0.9 ± 0.2
H β	-2.2 ± 0.9	-0.7 ± 0.8	-2.6 ± 0.1	-0.8 ± 0.1
[O III] $\lambda 5007$	0.3 ± 0.1	-0.7 ± 0.1	0.27 ± 0.02	-1.07 ± 0.02
H α + [N II]	-0.58 ± 0.06	-0.57 ± 0.06	-1.02 ± 0.02	-0.60 ± 0.02

NOTE.—The errors quoted are statistical only. For the strongest lines continuum-setting errors dominate.

internal agreement with all three of our data sets giving rather different values, but it is easy to see why. The very highly polarized Fe II emission makes the measurement interval setting, the continuum placement, and the assignment of local continuum polarization very difficult in that part of the spectrum. The Angel *et al.* H α + [N II] polarization is lower than ours, as was their continuum polarization in the red. (They found that the polarization of H α alone is $1.29\% \pm 0.15\%$, assuming the [N II] lines were polarized like $\lambda 5007$, and that they contribute 40% of the flux of the blend. Repeating their calculation with a modern value of 70% for the [N II] contribution [Koski 1978], but using their data, we find that H α alone has 2.6% polarization. This is as high as their H β value and in disagreement with their local continuum.) McLean *et al.* do give one line polarization, $Q = 0.7 \pm 0.2$ and $U = -1.1 \pm 0.2$ for [O III] $\lambda 5007$. This is similar to our result but rotated upward by a few degrees. Perhaps this reflects the position angle calibration difference seen in the continuum measurements.

REFERENCES

- Aannestad, P. A. 1975, *Ap. J.*, **200**, 30.
 Angel, J. R. P., Stockman, H. S., Woolf, N. J., Beaver, E. A., and Martin, P. G. 1976, *Ap. J. (Letters)*, **206**, L5.
 Antonucci, R. R. J. 1983, *Nature*, **303**, 158.
 ———. 1984, *Ap. J.*, **278**, 499.
 Antonucci, R. R. J., and Miller, J. S. 1984, *Bull. AAS*, **16**, 957.
 Balick, B., and Heckman, T. 1979, *A.J.*, **84**, 302.
 Bergeat, J., Lefevre, J., Kandel, R., Lunel, M., and Sibille, F. 1976, *Astr. Ap.*, **52**, 245.
 Blumenthal, G. R., Keel, W. C., and Miller, J. S. 1982, *Ap. J.*, **257**, 499.
 Chandrasekhar, S. 1946, *Ap. J.*, **103**, 351.
 Cohen, R. D. 1983, *Ap. J.*, **273**, 489.
 Elvius, A. 1978, *Astr. Ap.*, **65**, 233.
 Hildebrand, R. H., Whitcomb, S. E., Winston, R., Steining, R. F., Harper, D. A., and Moseley, S. H. 1977, *Ap. J.*, **216**, 698.
 Hiltner, W. A. 1956, *Ap. J. Suppl.*, **2**, 389.
 Koski, A. T. 1978, *Ap. J.*, **223**, 56.
 Kruszewski, A. 1971, *A.J.*, **76**, 576.
 Kwan, J. 1984, *Ap. J.*, **283**, 70.
 Lawrence, A., and Elvis, M. 1982, *Ap. J.*, **256**, 410.
 Lebofsky, M. J., Rieke, G. H., and Kemp, J. C. 1978, *Ap. J.*, **222**, 95.
 Malkan, M. A., and Filippenko, A. V. 1983, *Ap. J.*, **275**, 477.
 Malkan, M. A., and Oke, J. B. 1983, *Ap. J.*, **265**, 92.
 McLean, I. S., Aspin, C., Heathcote, S. R., and McCaughrean, M. J. 1983, *Nature*, **304**, 609.
 Meaburn, J., Morgan, B. L., Vine, H., Pedlar, A., and Spencer, R. 1982, *Nature*, **296**, 331.
 Miller, J. S., and Antonucci, R. R. J. 1983, *Ap. J. (Letters)*, **271**, L7 (Paper I).
 Miller, J. S., Robinson, L. B., and Schmidt, G. D. 1980, *Pub. A.S.P.*, **92**, 702.
 Neugebauer, G., *et al.* 1980, *Ap. J.*, **238**, 502.
 Ney, E. P., and Hatfield, B. F. 1978, *Ap. J. (Letters)*, **219**, L111.
 Pelat, D., and Alloin, D. 1980, *Astr. Ap.*, **81**, 172.
 Rieke, G. H. 1984, in *Astrophysics of Active Galaxies and Quasi-stellar Objects* (Mill Valley, Ca.: University Science Books), in press.
 Rieke, G. H., and Low, F. J. 1975, *Ap. J. (Letters)*, **199**, L13.
 Schmidt, G. D., and Miller, J. S. 1980, *Ap. J.*, **240**, 759.
 ———. 1985, *Ap. J.*, **290**, 517.
 Shields, G. A., and Oke, J. B. 1975, *Ap. J.*, **197**, 5.
 Shuder, J. M. 1981, *Ap. J.*, **244**, 12.
 The, P. S., *et al.* 1981, *Astr. Ap. Suppl.*, **44**, 451.
 Thompson, I., Landstreet, J. D., Stockman, H. S., Angel, J. R. P., and Beaver, E. A. 1980, *M.N.R.A.S.*, **192**, 53.
 Ulvestad, J. S., and Wilson, A. S. 1984, *Ap. J.*, **285**, 439.
 Visvanathan, N., and Oke, J. B. 1968, *Ap. J. (Letters)*, **152**, L165.
 Walker, M. F. 1968, *Ap. J.*, **151**, 71.
 Wampler, E. J. 1971, *Ap. J.*, **164**, 1.

R. R. J. ANTONUCCI: National Radio Astronomy Observatory, Edgemont Road, Charlottesville, VA 22903

J. S. MILLER: Lick Observatory, Board of Studies in Astronomy and Astrophysics, University of California, Santa Cruz, CA 95064